FAST-WAVE ANALYSIS OF AN INHOMOGENEOUSLY-LOADED HELIX ENCLOSED IN A CYLINDRICAL WAVEGUIDE

S. Ghosh, P. K. Jain, and B. N. Basu

Centre of Research in Microwave Tubes
Department of Electronics Engineering
Institute of Technology
Banaras Hindu University
Varanasi - 221 005, India

1. INTRODUCTION

The helix, which is a non-resonant electromagnetic structure, finds applications as an antenna [1], a delay line [2], an applicator in hyperthermia [3] and as a slow-wave structure in a wide-band traveling-wave tube (TWT). Such a helix — held in position in a TWT by a dielectric-support system enclosed in an envelope, say, made of metal — was analyzed in the past through mostly in the slow-wave regime [4–8]. However, more recently, Uhm and Choe [9–11] extended the analysis of such a structure in the fast-wave regime keeping in mind its potential application in a gyro-resonance electron beam device like the gyro-TWT — an upcoming high-power, millimeter-wave amplifier for communication systems. The objective was to control the structure parameters with a view to shaping the dispersion (ω-β) characteristics

of the structure for a wide-band coalescence between the beam-mode dispersion line and the waveguide-mode dispersion hyperbola. In analyzing the structure, however, Uhm and Choe [9, 10] ignored the effects of the dielectric-support system for the helix, though they considered the effects of the proximity of a metal envelope — the conventional cylindrical waveguide. Here, we have considered in the analysis the effects of the dielectric-support parameters, including the inhomogeneity of the dielectric, in addition to the helix-envelope separation, on the dispersion and interaction impedance characteristics of the structure.

In the following section is developed the analysis of a helix closely fitting in a dielectric lining on the inner wall of a cylindrical waveguide — a structure that presents a 'homogeneous' loading for the helix. Moreover, we also analyze a helix supported by a number of identical discrete dielectric rods/bars, arranged symmetrically around the helix, in the waveguide. Such a support system now presents, in general, an 'inhomogeneous' loading for the helix which in turn loads the waveguide internally. The inhomogeneity in such a structure is determined by the cross-sectional geometry of the dielectric supports for the helix. In the analytical model used here, the discrete inhomogeneous dielectric supports are azimuthally smoothed out into a number of continuous, homogeneous dielectric tube regions. For a particular case of wedge-shaped dielectric supports, a field analysis was earlier carried out considering azimuthal space harmonics generated by their angular periodicity [8]. Hence it was also established that such discrete wedge supports may be azimuthally smoothed out into a single equivalent continuous, homogeneous dielectric tube of an effective permittivity determined by the relative volume occupied by the supports in the structure [8]. Such wedge supports thus present essentially a homogeneous loading for the helix. However, the supports in general could deviate from simple wedge geometry. For this situation the present approach of smearing out the discrete supports into a number of equivalent dielectric tube regions, instead of a single region, would be a reasonably good approximation, if the number of such regions is considered large enough to yield converging results. Furthermore, in order to take into account the space-harmonic effects we use the tape model for the helix [2, 12, 13]. Also, in order to add to the rigor of analysis, we consider the effects of the finite helix thickness as well as those of the non-uniformity of the radial propagation constant over the various cross-sectional regions of the structure. The analysis of

the structure is then used to study the dispersion characteristics of the structure as well as to examine its quality in terms of the interaction impedance [14, 15] — a quantity which is relevant to the application of such a structure in an electron beam device like the gyro-TWT, which uses an 'azimuthal' electron beam bunching and beam-wave interaction mechanism. It may be mentioned that attempts have been made here to present the analytical results in a simplified form involving structured expressions which are easy to handle and amenable to easy computation requiring less computer time for any desired convergence accuracy.

2. ANALYSIS

Let us consider a helix supported by a number of identical discrete dielectric bars/rods of an arbitrary cross section in a cylindrical waveguide (Fig. 1a). Such a support geometry in general causes an inhomogeneous structure loading and may be analyzed in a model in which the discrete supports are azimuthally smoothed out into n continuous dielectric tube regions of appropriate 'effective' permittivity values determined by the relative volume occupied by the supports in the structure (see the discussion following (1)) — the value of n increased for the desired convergence accuracy [16] (Fig. 1b). It may be noted that, here, the helix presents a skew boundary in the structure thereby arousing both TE and TM modes. Further, the space periodicity of the helix has been accounted for in the analysis by using the tape-helix [2, 12, 13] instead of the simplified sheath-helix model [17]. Moreover, the usual approximation made in analyzing a loaded helical structure by considering the radial propagation constant to be the same in the different structure regions is removed here by taking into account the nonuniformity of the radial propagation constant over the structure cross section. Considering the RF quantities associated with the m th space-harmonic mode to vary as $\exp j(\omega t - \beta_m z + m\theta)$, one may write the following expressions for the components of the electric (E) and magnetic (H) field intensities in the different structure regions in the cylindrical system of coordinates (r, θ, z):
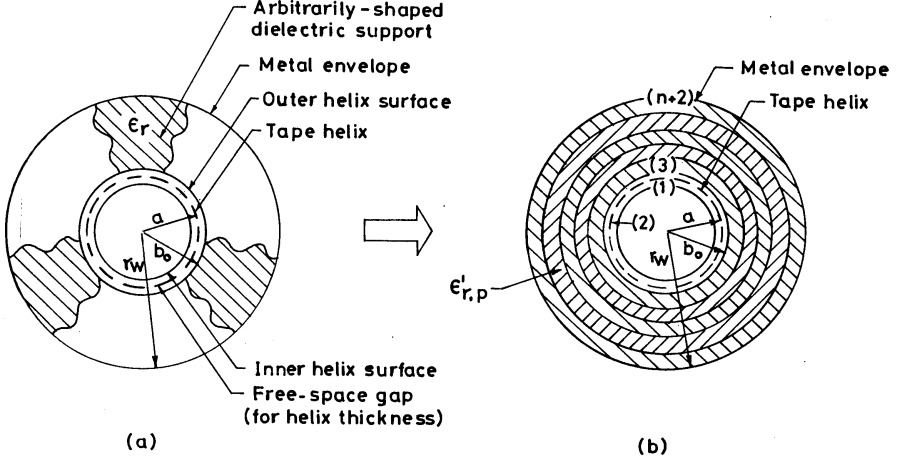
Figure 1. Cross section of an inhomogeneously-loaded helix supported by arbitrarily-shaped dielectric bars **(a)** and its equivalent model **(b)**.

$$E_{z,p} = \sum_{m=-\infty}^{\infty} E_{z,m,p} = \sum_{m=-\infty}^{\infty} \left(A_{m,p} J_m \left\{ \gamma_{m,p} r \right\} + B_{m,p} Y_m \left\{ \gamma_{m,p} r \right\} \right),$$

$$H_{z,p} = \sum_{m=-\infty}^{\infty} H_{z,m,p} = \sum_{m=-\infty}^{\infty} \left(C_{m,p} J_m \left\{ \gamma_{m,p} r \right\} + D_{m,p} Y_m \left\{ \gamma_{m,p} r \right\} \right),$$

$$E_{\theta,p} = \sum_{m=-\infty}^{\infty} E_{\theta,m,p}$$

$$= \sum_{m=-\infty}^{\infty} \left[\frac{m\beta_m}{r\gamma_{m,p}^2} \left(A_{m,p} J_m \left\{ \gamma_{m,p} r \right\} + B_{m,p} Y_m \left\{ \gamma_{m,p} r \right\} \right) \right.$$

$$\left. + \frac{j\omega\mu_0}{\gamma_{m,p}} \left(C_{m,p} J_m' \left\{ \gamma_{m,p} r \right\} + D_{m,p} Y_m' \left\{ \gamma_{m,p} r \right\} \right) \right],$$

$$H_{\theta,p} = \sum_{m=-\infty}^{\infty} H_{\theta,m,p}$$

$$= \sum_{m=-\infty}^{\infty} \left[-\frac{j\omega\epsilon_0 \epsilon_{r,p}'}{\gamma_{m,p}} \left(A_{m,p} J_m' \left\{ \gamma_{m,p} r \right\} + B_{m,p} Y_m' \left\{ \gamma_{m,p} r \right\} \right) \right.$$

$$\left. + \frac{m\beta_m}{r\gamma_{m,p}^2} \left(C_{m,p} J_m \left\{ \gamma_{m,p} r \right\} + D_{m,p} Y_m \left\{ \gamma_{m,p} r \right\} \right) \right],$$

$$E_{r,p} = \sum_{m=-\infty}^{\infty} E_{r,m,p}$$

$$= \sum_{m=-\infty}^{\infty} \left[-\frac{j\beta_m}{\gamma_{m,p}} \left(A_{m,p} J'_m \{\gamma_{m,p}r\} + B_{m,p} Y'_m \{\gamma_{m,p}r\} \right) \right.$$

$$\left. + \frac{m\omega\mu_0}{r\gamma_{m,p}^2} \left(C_{m,p} J_m \{\gamma_{m,p}r\} + D_{m,p} Y_m \{\gamma_{m,p}r\} \right) \right],$$

and

$$H_{r,p} = \sum_{m=-\infty}^{\infty} H_{r,m,p}$$

$$= -\sum_{m=-\infty}^{\infty} \left[\frac{m\omega\epsilon_0\epsilon'_{r,p}}{r\gamma_{m,p}^2} \left(A_{m,p} J_m \{\gamma_{m,p}r\} + B_{m,p} Y_m \{\gamma_{m,p}r\} \right) \right.$$

$$\left. + \frac{j\beta_m}{\gamma_{m,p}} \left(C_{m,p} J'_m \{\gamma_{m,p}r\} + D_{m,p} Y'_m \{\gamma_{m,p}r\} \right) \right], \quad (1)$$

where p refers to a region of the structure (Fig. 1b). $A_{m,p}$, $B_{m,p}$, $C_{m,p}$, and $D_{m,p}$ are the field constants. $\gamma_{m,p}(= (k^2\epsilon'_{r,p} - \beta_m^2)^{1/2})$ is the radial propagation constant, $k(= \omega(\mu_0\epsilon_0)^{1/2})$ and $\beta_m(= \beta_0 + m\cot\psi/a)$ being the free-space and the axial propagation constants of the structure, respectively. ψ and a are the pitch angle and the mean radius of the helix, and $\epsilon'_{r,p}(= 1 + (\epsilon_r - 1)\hat{A}_{sp}/\hat{A}_p)$ represents the effective relative permittivity [16] of the pth of the n effective dielectric tube regions into which the discrete supports are azimuthally smoothed out (Fig. 1), $\hat{A}_p$ being the cross-sectional area of the entire pth tube, $\hat{A}_{sp}$ the cross-sectional area of the actual dielectric supports in the pth tube region, and ϵ_r the relative permittivity of the support material. m represents the space harmonic number. $J_m \{\gamma_{m,p}r\}$ and $Y_m \{\gamma_{m,p}r\}$ represent the Bessel functions of order m of the first and second kinds, respectively, the prime indicating their derivative with respect to the argument.

2.1. Circuit Dispersion

The structure model for analysis has $(n+2)$ regions (Fig. 1b): the free-space region $(p = 1, \epsilon'_{r,1} = 1, 0 < r < a)$ inside the winding radius $(r = a)$ of the helical tape, the free-space gap $(p = 2, \epsilon'_{r,2} = 1, a < r < b_0)$ between the tape and the beginning $(r = b_0)$ of the

dielectric regions, to take into account the finite helix wire/tape thickness [18] $(= 2(b_0 - a))$, and n continuous, homogeneous, effective dielectric tube regions into which the discrete helix supports are azimuthally smoothed out. Out of $(4n + 8)$ field constants relevant to these $(n + 2)$ regions, $B_{m,1}$ and $D_{m,1}$ become each equal to zero to satisfy the condition that the fields are to be finite at the axis $(r = 0)$ of the structure, giving $(4n + 6)$ non-zero field constants. The relevant electromagnetic boundary conditions for the problem are: the tape-helix boundary conditions [12] at $r = a$, the boundary conditions related to the continuity of the tangential components of the electric and magnetic field intensities at each of the interfaces $(r = b_p)$ between the dielectric tube regions (between the pth and $(p + 1)$th), and the boundary condition that the tangential component of electric field intensity is null at the waveguide wall $(r = b_n = r_W)$. These boundary conditions are:

at $r = a$:

$$E_{1,\parallel} = \sum_{m=-\infty}^{\infty} E_{1,\parallel,m} = \sum_{m=-\infty}^{\infty} (E_{\theta,1,m} \cos \psi + E_{z,1,m} \sin \psi) = 0,$$

$$E_{2,\parallel} = \sum_{m=-\infty}^{\infty} E_{2,\parallel,m} = \sum_{m=-\infty}^{\infty} (E_{\theta,2,m} \cos \psi + E_{z,2,m} \sin \psi) = 0,$$

$$E_{z,1,m} = E_{z,2,m},$$

$$E_{\theta,1,m} = E_{\theta,2,m},$$

$$H_{z,1,m} - H_{z,2,m} = J_{\theta,m} = J_{\parallel,m} \cos \psi,$$

$$H_{\theta,2,m} - H_{\theta,1,m} = J_{z,m} = J_{\parallel,m} \sin \psi,$$

$$J_{\theta,m} \sin \psi - J_{z,m} \cos \psi = 0;$$

at $r = b_p$:

$$E_{z,p} = E_{z,p+1}, \quad E_{\theta,p} = E_{\theta,p+1},$$

$$H_{z,p} = H_{z,p+1}, \quad H_{\theta,p} = H_{\theta,p+1};$$

at $r = b_n = r_W$:

$$E_{z,n+1} = 0, \quad E_{\theta,n+1} = 0.$$

With the help of these boundary conditions, one may choose to express the field constants in terms of a single constant, namely, $A_{m,1}$. Then following the Sensiper's approach [12], one may express $A_{m,1}$ in terms of the amplitude of the mth harmonic Fourier component of the tape surface current density in the direction of the tape, which in turn may be easily found assuming a simple tape-current distribution, with all its Fourier components summed together—by taking it constant in amplitude over the tape width and varying in phase along the helix winding direction as per the phase propagation constant of the fundamental mode [2, 12] as follows:

$$A_{m,1} = \zeta_1 J_{\parallel,m}$$

with ζ_1 defined in Appendix. Next, the electric field intensity parallel to the winding direction at the center line of the tape $E_{1,\parallel}(a)(z = p\theta/2\pi)$, is expressed in terms of $A_{m,1}$, and hence in terms of the assumed current distribution. Precisely, thus one gets $E_{1,\parallel}(a)(z = p\theta/2\pi)$ in terms of J, being the amplitude of $J_{\parallel}(= J\exp(-j\beta_0 z))$, the latter expanded into its Fourier components as:

$$J_{\parallel} = \exp(-j\beta_0 z) \sum_{m=-\infty}^{\infty} J\left(\frac{\sin(\beta_m\delta/2)}{(\beta_m\delta/2)}\right)\left(\frac{\delta}{p}\right)\exp[-jn(2\pi z/p - \theta)].$$

$E_{1,\parallel}(a)(z = p\theta/2\pi)$, thus obtained in terms of J, is set equal to zero to obtain the dispersion relation in the following simplified form after a lengthy algebra:

$$\sum_{m=-\infty}^{\infty}\left[\left(1 + \frac{m\beta_m\cot\psi}{\gamma_m^2 a}\right)^2\left(1 + \frac{Q_0 J_m\{\gamma_m a\}}{P_0 Y_m\{\gamma_m a\}}\right) \times \right.$$
$$\left(1 + \frac{N_0 J'_m\{\gamma_m a\}}{M_0 Y'_m\{\gamma_m a\}}\right)^{-1}\left(\frac{J_m\{\gamma_m a\} Y_m\{\gamma_m a\}}{J'_m\{\gamma_m a\} Y'_m\{\gamma_m a\}}\right)$$
$$\left. + \left(\frac{k\cot\psi}{\gamma_m}\right)^2\right]\left(\frac{\sin(\beta_m\delta/2)}{\beta_m\delta/2}\right) = 0, \tag{2}$$

where $\gamma_m(= \gamma_{m,1} = \gamma_{m,2}) = (k^2 - \beta_m^2)^{1/2}$ is the radial propagation constant of the free-space region. δ is the width of the tape. P_0, Q_0, M_0, and N_0 can be found from the following recurrence relations:

for $2 \leq p \leq n$:

$$
\begin{aligned}
P_{p-2} = \\
\Bigg[&\left(\epsilon'_{r,p} \frac{Y_m \left\{\gamma_{m,p+1} b_{p-2}\right\}}{J_m \left\{\gamma_{m,p} b_{p-2}\right\}} - \frac{\gamma_{m,p}}{\gamma_{m,p+1}} \epsilon'_{r,p+1} \frac{Y'_m \left\{\gamma_{m,p+1} b_{p-2}\right\}}{J'_m \left\{\gamma_{m,p} b_{p-2}\right\}} \right) P_{p-1} \\
+ &\left(\epsilon'_{r,p} \frac{J_m \left\{\gamma_{m,p+1} b_{p-2}\right\}}{J_m \left\{\gamma_{m,p} b_{p-2}\right\}} - \frac{\gamma_{m,p}}{\gamma_{m,p+1}} \epsilon'_{r,p+1} \frac{J'_m \left\{\gamma_{m,p+1} b_{p-2}\right\}}{J'_m \left\{\gamma_{m,p} b_{p-2}\right\}} \right) Q_{p-1} \\
- &\frac{m\beta_m}{\omega \epsilon_0 b_p \gamma_{m,p}} \left(1 - \frac{\gamma_{m,p}^2}{\gamma_{m,p+1}^2} \right) \times \\
&\left(\frac{M_{p-1} Y_m \left\{\gamma_{m,p+1} b_{p-2}\right\} + N_{p-1} J_m \left\{\gamma_{m,p+1} b_{p-2}\right\}}{J'_m \left\{\gamma_{m,p} b_{p-2}\right\}} \right) \Bigg] \times \\
&J_m \left\{\gamma_{m,p} b_{p-2}\right\} J'_m \left\{\gamma_{m,p} b_{p-2}\right\},
\end{aligned}
\tag{3}
$$

$$
\begin{aligned}
Q_{p-2} = \\
-\Bigg[&\left(\epsilon'_{r,p} \frac{Y_m \left\{\gamma_{m,p+1} b_{p-2}\right\}}{Y_m \left\{\gamma_{m,p} b_{p-2}\right\}} - \frac{\gamma_{m,p}}{\gamma_{m,p+1}} \epsilon'_{r,p+1} \frac{Y'_m \left\{\gamma_{m,p+1} b_{p-2}\right\}}{Y'_m \left\{\gamma_{m,p} b_{p-2}\right\}} \right) P_{p-1} \\
+ &\left(\epsilon'_{r,p} \frac{J_m \left\{\gamma_{m,p+1} b_{p-2}\right\}}{Y_m \left\{\gamma_{m,p} b_{p-2}\right\}} - \frac{\gamma_{m,p}}{\gamma_{m,p+1}} \epsilon'_{r,p+1} \frac{J'_m \left\{\gamma_{m,p+1} b_{p-2}\right\}}{Y'_m \left\{\gamma_{m,p} b_{p-2}\right\}} \right) Q_{p-1} \\
- &\frac{m\beta_m}{\omega \epsilon_0 b_{p-2} \gamma_{m,p}} \left(1 - \frac{\gamma_{m,p}^2}{\gamma_{m,p+1}^2} \right) \times \\
&\left(\frac{M_{p-1} Y_m \left\{\gamma_{m,p+1} b_{p-2}\right\} + N_{p-1} J_m \left\{\gamma_{m,p+1} b_{p-2}\right\}}{Y'_m \left\{\gamma_{m,p} b_{p-2}\right\}} \right) \Bigg] \times \\
&Y_m \left\{\gamma_{m,p} b_{p-2}\right\} Y'_m \left\{\gamma_{m,p} b_{p-2}\right\},
\end{aligned}
\tag{4}
$$

$$
\begin{aligned}
M_{p-2} = \\
\Bigg[&\left(\frac{Y_m \left\{\gamma_{m,p+1} b_{p-2}\right\}}{J_m \left\{\gamma_{m,p} b_{p-2}\right\}} - \frac{\gamma_{m,p}}{\gamma_{m,p+1}} \frac{Y'_m \left\{\gamma_{m,p+1} b_{p-2}\right\}}{J'_m \left\{\gamma_{m,p} b_{p-2}\right\}} \right) M_{p-1} \\
+ &\left(\frac{J_m \left\{\gamma_{m,p+1} b_{p-2}\right\}}{J_m \left\{\gamma_{m,p} b_{p-2}\right\}} + \frac{\gamma_{m,p}}{\gamma_{m,p+1}} \frac{J'_m \left\{\gamma_{m,p+1} b_{p-2}\right\}}{J'_m \left\{\gamma_{m,p} b_{p-2}\right\}} \right) N_{p-1} \\
+ &\frac{m\beta_m}{\omega \mu_0 b_{p-2} \gamma_{m,p}} \left(1 - \frac{\gamma_{m,p}^2}{\gamma_{m,p+1}^2} \right) \times
\end{aligned}
$$

$$\left(\frac{P_{p-1} Y_m \{\gamma_{m,p+1} b_{p-2}\} + Q_{p-1} J_m \{\gamma_{m,p+1} b_{p-2}\}}{J'_m \{\gamma_{m,p} b_{p-2}\}} \right) \Bigg] \times$$
$$J_m \{\gamma_{m,p} b_{p-2}\} J'_m \{\gamma_{m,p} b_{p-2}\}, \tag{5}$$

and

$$N_{p-2} =$$
$$-\Bigg[\left(\frac{Y_m \{\gamma_{m,p+1} b_{p-2}\}}{Y_m \{\gamma_{m,p} b_{p-2}\}} - \frac{\gamma_{m,p}}{\gamma_{m,p+1}} \frac{Y'_m \{\gamma_{m,p+1} b_{p-2}\}}{Y'_m \{\gamma_{m,p} b_{p-2}\}} \right) M_{p-1}$$
$$+ \left(\frac{J_m \{\gamma_{m,p+1} b_{p-2}\}}{Y_m \{\gamma_{m,p} b_{p-2}\}} - \frac{\gamma_{m,p}}{\gamma_{m,p+1}} \frac{J'_m \{\gamma_{m,p+1} b_{p-2}\}}{Y'_m \{\gamma_{m,p} b_{p-2}\}} \right) N_{p-1}$$
$$+ \frac{m\beta_m}{\omega\mu_0 b_{p-2}\gamma_{m,p}} \left(1 - \frac{\gamma_{m,p}^2}{\gamma_{m,p+1}^2} \right) \times$$
$$\left(\frac{P_{p-1} Y_m \{\gamma_{m,p+1} b_{p-2}\} + Q_{p-1} J_m \{\gamma_{m,p+1} b_{p-2}\}}{Y'_m \{\gamma_{m,p} b_{p-2}\}} \right) \Bigg] \times$$
$$Y_m \{\gamma_{m,p} b_{p-2}\} Y'_m \{\gamma_{m,p} b_{p-2}\}, \tag{6}$$

where b_p is the outer radius of the pth dielectric tube (Fig. 1b).

With the help of (3)–(6), P_0, Q_0, M_0, and N_0 are obtained in terms of P_{n-1}, Q_{n-1}, M_{n-1}, and N_{n-1} which, in turn, are given by:

$$P_{n-1} = J_m \{\gamma_{m,n+1} b_{n-1}\} Y_m \{\gamma_{m,n+2} b_{n-1}\}$$
$$\Bigg[\frac{\gamma_{m,n+1}}{\gamma_{m,n+2}} \epsilon'_{r,n+2} \left(1 - \frac{J'_m \{\gamma_{m,n+2} b_{n-1}\} Y_m \{\gamma_{m,n+2} r_W\}}{Y'_m \{\gamma_{m,n+2} b_{n-1}\} J_m \{\gamma_{m,n+2} r_W\}} \right) \times$$
$$\frac{Y'_m \{\gamma_{m,n+2} b_{n-1}\}}{Y_m \{\gamma_{m,n+2} b_{n-1}\}}$$
$$- \epsilon'_{r,n+1} \left(1 - \frac{J_m \{\gamma_{m,n+2} b_{n-1}\} Y_m \{\gamma_{m,n+2} r_W\}}{Y_m \{\gamma_{m,n+2} b_{n-1}\} J_m \{\gamma_{m,n+2} r_W\}} \right) \times$$
$$\frac{J'_m \{\gamma_{m,n+1} b_{n-1}\}}{J_m \{\gamma_{m,n+1} b_{n-1}\}}$$
$$- \frac{m\beta_m \gamma_m (1 - \gamma_{m,n+1}^2/\gamma_{m,n+2}^2)}{\omega^2 \mu_0 \epsilon_0 \cot\psi \epsilon'_{r,n} \epsilon'_{r,n+1} b_{n-1} \gamma_{m,n+1}} \times$$
$$\left(\frac{P_0 Y_m \{\gamma_m a\} + Q_0 J_m \{\gamma_m a\}}{M_0 Y'_m \{\gamma_m a\} + N_0 J'_m \{\gamma_m a\}} \right) \times$$
$$\left(1 - \frac{J_m \{\gamma_{m,n+2} b_{n-1}\} Y'_m \{\gamma_{m,n+2} r_2\}}{Y_m \{\gamma_{m,n+2} b_{n-1}\} J'_m \{\gamma_{m,n+2} r_2\}} \right) \Bigg], \tag{7}$$

$$Q_{n-1} = -Y_m \left\{ \gamma_{m,n+1} b_{n-1} \right\} Y_m \left\{ \gamma_{m,n+2} b_{n-1} \right\}$$
$$\left[\frac{\gamma_{m,n+1}}{\gamma_{m,n+2}} \epsilon'_{r,n+2} \left(1 - \frac{J'_m \left\{ \gamma_{m,n+2} b_{n-1} \right\} Y_m \left\{ \gamma_{m,n+2} r_W \right\}}{Y'_m \left\{ \gamma_{m,n+2} b_{n-1} \right\} J_m \left\{ \gamma_{m,n+2} r_W \right\}} \right) \times \right.$$
$$\frac{Y'_m \left\{ \gamma_{m,n+2} b_{n-1} \right\}}{Y_m \left\{ \gamma_{m,n+2} b_{n-1} \right\}}$$
$$- \epsilon'_{r,n+1} \left(1 - \frac{J_m \left\{ \gamma_{m,n+2} b_{n-1} \right\} Y_m \left\{ \gamma_{m,n+2} r_W \right\}}{Y_m \left\{ \gamma_{m,n+1} b_{n-1} \right\} J_m \left\{ \gamma_{m,n+2} r_W \right\}} \right) \times$$
$$\frac{Y'_m \left\{ \gamma_{m,n+1} b_{n-1} \right\}}{Y_m \left\{ \gamma_{m,n+1} b_{n-1} \right\}}$$
$$- \frac{m \beta_m \gamma_m (1 - \gamma^2_{m,n+1}/\gamma^2_{m,n+2})}{\omega^2 \mu_0 \epsilon_0 \cot \psi \epsilon'_{r,n} \epsilon'_{r,n+1} b_{n+1} \gamma_{m,n+1}} \times$$
$$\left(\frac{P_0 Y_m \left\{ \gamma_m a \right\} + Q_0 J_m \left\{ \gamma_m a \right\}}{M_0 Y'_m \left\{ \gamma_m a \right\} + N_0 J'_m \left\{ \gamma_m a \right\}} \right) \times$$
$$\left. \left(1 - \frac{J_m \left\{ \gamma_{m,n+2} b_{n-1} \right\} Y'_m \left\{ \gamma_{m,n+2} r_W \right\}}{Y_m \left\{ \gamma_{m,n+2} b_{n-1} \right\} J'_m \left\{ \gamma_{m,n+2} r_W \right\}} \right) \right], \qquad (8)$$

$$M_{n-1} = -J_m \left\{ \gamma_{m,n+1} b_{n-1} \right\} Y_m \left\{ \gamma_{m,n+2} b_{n-1} \right\} \times$$
$$\left[\frac{\gamma_{m,n+1}}{\gamma_{m,n+2}} \left(1 - \frac{J'_m \left\{ \gamma_{m,n+2} b_{n-1} \right\} Y'_m \left\{ \gamma_{m,n+2} r_W \right\}}{Y'_m \left\{ \gamma_{m,n+2} b_{n-1} \right\} J'_m \left\{ \gamma_{m,n+2} r_W \right\}} \right) \times \right.$$
$$\frac{Y'_m \left\{ \gamma_{m,n+2} b_{n-1} \right\}}{Y_m \left\{ \gamma_{m,n+2} b_{n-1} \right\}}$$
$$- \left(1 - \frac{J_m \left\{ \gamma_{m,n+2} b_{n-1} \right\} Y'_m \left\{ \gamma_{m,n+2} r_W \right\}}{Y_m \left\{ \gamma_{m,n+2} b_{n-1} \right\} J'_m \left\{ \gamma_{m,n+2} r_W \right\}} \right) \times$$
$$\frac{J'_m \left\{ \gamma_{m,n+1} b_{n-1} \right\}}{J_m \left\{ \gamma_{m,n+1} b_{n-1} \right\}}$$
$$- \frac{m \beta_m \epsilon'_{r,n} \epsilon'_{r,n+1} (1 - \gamma^2_{m,n+1}/\gamma^2_{m,n+2})}{\gamma_m b_{n-1} \gamma_{m,n+1}} \times$$
$$\left(\frac{M_0 Y'_m \left\{ \gamma_m a \right\} + N_0 J'_m \left\{ \gamma_m a \right\}}{P_0 Y_m \left\{ \gamma_m a \right\} + Q_0 J_m \left\{ \gamma_m a \right\}} \right) \times$$
$$\left. \left(1 - \frac{J_m \left\{ \gamma_{m,n+2} b_{n-1} \right\} Y_m \left\{ \gamma_{m,n+2} r_W \right\}}{Y_m \left\{ \gamma_{m,n+2} b_{n-1} \right\} J_m \left\{ \gamma_{m,n+2} r_W \right\}} \right) \right], \qquad (9)$$

$$N_{n-1} = Y_m \left\{ \gamma_{m,n+1} b_{n-1} \right\} Y_m \left\{ \gamma_{m,n+2} b_{n-1} \right\} \times$$
$$\left[\frac{\gamma_{m,n+1}}{\gamma_{m,n+2}} \left(1 - \frac{J'_m \left\{ \gamma_{m,n+2} b_{n-1} \right\} Y'_m \left\{ \gamma_{m,n+2} r_W \right\}}{Y'_m \left\{ \gamma_{m,n+2} b_{n-1} \right\} J'_m \left\{ \gamma_{m,n+2} r_W \right\}} \right) \times \right.$$
$$\frac{Y'_m \left\{ \gamma_{m,n+2} b_{n-1} \right\}}{Y_m \left\{ \gamma_{m,n+2} b_{n-1} \right\}}$$
$$- \left(1 - \frac{J_m \left\{ \gamma_{m,n+2} b_{n-1} \right\} Y'_m \left\{ \gamma_{m,n+1} r_W \right\}}{Y_m \left\{ \gamma_{m,n+2} b_{n-1} \right\} J'_m \left\{ \gamma_{m,n+1} r_W \right\}} \right) \times$$
$$\frac{Y'_m \left\{ \gamma_{m,n+1} b_{n-1} \right\}}{Y_m \left\{ \gamma_{m,n+1} b_{n-1} \right\}}$$
$$- \frac{m \beta_m \epsilon'_{r,n} \epsilon'_{r,n+1} (1 - \gamma^2_{m,n+1}/\gamma^2_{m,n+2})}{\gamma_m b_{n-1} \gamma_{m,n+1}} \times$$
$$\left(\frac{M_0 Y'_m \left\{ \gamma_m a \right\} + N_0 J'_m \left\{ \gamma_m a \right\}}{P_0 Y_m \left\{ \gamma_m a \right\} + Q_0 J_m \left\{ \gamma_m a \right\}} \right) \times$$
$$\left. \left(1 - \frac{J_m \left\{ \gamma_{m,n+2} b_{n-1} \right\} Y_m \left\{ \gamma_{m,n+2} r_W \right\}}{Y_m \left\{ \gamma_{m,n+2} b_{n-1} \right\} J_m \left\{ \gamma_{m,n+2} r_W \right\}} \right) \right]. \quad (10)$$

It may be seen from (3)–(6) that P_0, Q_0, M_0, and N_0 are each expressible in terms of P_{n-1}, Q_{n-1}, M_{n-1}, and N_{n-1}. However, it may also be seen from (7)–(10) that the latter each involve P_0, Q_0, M_0, and N_0 again. The approach one can follow here is to ignore the terms containing P_0, Q_0, M_0, and N_0 in the right hand side of (7)–(10), as a first order of approximation, to obtain the approximate values of P_{n-1}, Q_{n-1}, M_{n-1}, and N_{n-1}. Using these approximate values and with the help of (3)–(6) one may then approximately evaluate P_0, Q_0, M_0, and N_0 which can be substituted back into (7)–(10) to obtain more accurate values of P_{n-1}, Q_{n-1}, M_{n-1}, and N_{n-1}. The latter in turn can again be used in (3)–(6) to evaluate the values of P_0, Q_0, M_0, and N_0, more accurately. The method is iterated till each of the values of P_0, Q_0, M_0, and N_0 converges. Subsequently, these values can be used in the dispersion relation (2) for the desired dispersion characteristics of the structure. It will be of interest to check that, as a special case in which the effects of the dielectric support for the helix are ignored, the dispersion relation (2) would pass on to that of Uhm and Choe [10].

2.2 Circuit Impedance

The quality of the structure analyzed in providing the RF electric field for interaction with an electron beam in a practical device can be estimated in terms of the interaction impedance of the structure [13, 14, 17]. For a tenuous annular electron beam, in a fast-wave device like the gyro-TWT, the effect of the presence of the beam on the spatial texture of the waveguide may be ignored. One may then define $K_{\theta,m}$, the azimuthal interaction impedance of the mth space-harmonic mode, as [14, 15]:

$$K_{\theta,m} = \frac{E_{\theta,m}^2 \{r_{\text{beam}}\}}{2\beta_m^2 \mathcal{P}} \tag{11}$$

where $E_{\theta,m}\{r_{\text{beam}}\}$ is the azimuthal component of electric field intensity of the mth space-harmonic mode at the mean beam position $(r = r_{\text{beam}})$, it being assumed that in such a device the azimuthal component of electric field intensity is predominantly responsible for interaction with a thin annular beam of electrons in helical trajectories. $\mathcal{P}$ is the power propagating down the structure, which is found by taking half of the real part of the integration of the complex Poynting vector over the cross-sectional area of the structure for all the space harmonic modes summed up together. Substituting $\mathcal{P}$ thus found in (11), one obtains:

$$K_{\theta,m} = \frac{E_{\theta,m}^2 \{r_{\text{beam}}\}}{2\beta_m^2 \sum_{m=-\infty}^{\infty} \sum_{p=1}^{p+2} G_{m,p}} \tag{12}$$

where $G_{m,p}$ are the functions of the structure parameters as given in Appendix.

3. RESULTS AND DISCUSSION

In this paper we present an analytical method to study a general helix-loaded structure— an inhomogeneously-loaded helix enclosed in a cylindrical waveguide operating in the fast-wave regime. The tape-helix model has been used which takes into account the effect of the space-harmonics, as it is particularly relevant to situations in which the structure is operated at high voltages and for high helix pitch angles.

In the analytical model, the structure inhomogeneity has been modeled by azimuthally smoothing out the discrete supports into a number of continuous dielectric tube regions of the appropriate permittivity values (Fig. 1). The number of such simulated continuous homogeneous dielectric tube regions is increased usually up to $\sim$ 10 or 15, for converging results. The effect of helix tape thickness is taken into account to add to the practical relevance of the problem. The non-uniformity in the radial propagation constant in the different structure regions is considered, particularly for a large structure inhomogeneity caused by a high-permittivity support for the helix, a large separation between the helix and the waveguide wall, and for large helix pitch angles [19, 20]. The structured expressions presented, which are amenable to easy computation with the help of relevant recurrence relations, enable one to use them easily in an iterative cycle for the desired convergence accuracy, as discussed following (10). The solution involves the usual bisection followed by Muller's method. The entire iteration hardly took a couple of seconds to obtain a value each of normalized axial phase propagation constant and interaction impedance, for a given normalized frequency and a set of input structure parameters, on an IBM-compatible Pentium based PC-AT.

For the numerical appreciation of the problem, the dispersion and the impedance versus frequency characteristics are plotted for a homogenerously-loaded helix $(\epsilon'_{r,p}/\epsilon'_{r,p-1} = 1; p \geq 3)$ taking a/r_w, the size of the helix relative to that of the waveguide (Fig. 2a), $\cot\psi$ the cotangent of the helix pitch angle (Fig. 2b), and $\epsilon'_r (= \epsilon'_{r,3} = \epsilon'_{r,4} = \ldots)$, the effective relative permittivity of the support regions (Fig. 2c) as the parameters. The same characteristics are also plotted for an inhomogeneously-loaded helix $(\epsilon'_{r,p}/\epsilon'_{r,p-1} \neq 1; p \geq 3)$ taking $\epsilon'_{r,p}/\epsilon'_{r,p-1}$, the structure inhomogeneity factor, considered as uniform over the support cross-section, (Fig. 2d) as the parameter. For this purpose, the lowest-order solution for the hybrid-mode relation (2) is taken.

The structure loading increases giving a larger value of β_0, as the helix is moved farther from or closer to the waveguide wall depending on whether the helix has a dielectric support or not (Fig. 2a) and for a higher permittivity helix support (Fig. 2c). Furthermore, for an inhomogeneously-loaded structure, the loading increases with the inhomogeneity if the permittivity increases radially outward $(\epsilon'_{r,p}/\epsilon'_{r,p-1} > 1)$, while it decreases if the permittivity decreases radially outward
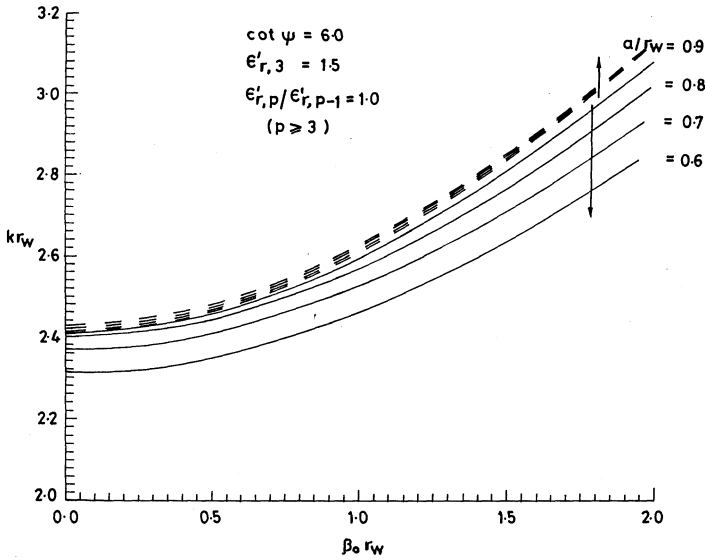
Figure 2(a). Dispersion characteristics — kr_w, a normalized frequency, versus βr_w, a normalized phase propagation constant of the fundamental mode $(m = 0)$, plotted for a homogeneously-loaded structure taking the following parameters: a/r_w **(a)**, $\cot \psi$ **(b)**, and $\epsilon'_{r,3}$ **(c)**; and the same characteristics plotted for an inhomogeneously-loaded structure taking $\epsilon'_{r,p}/\epsilon'_{r,p-1}$, considered as uniform, as the parameter **(d)** — the solid line referring to the permittivity increasing radially outward, the solid line with crosses to the permittivity increasing radially inward, and the broken line with circles to the homogeneous dielectric loading, the thickness of the tape being ignored $(b_0 = a)$, thought its width considered at a normalized value $\delta/p = 0.3$, the broken line referring to the dielectric-free $(\epsilon'_{r,3} = 1)$ structure [9], [10] in **(a)**–**(d)**.

$(\epsilon'_{r,p}/\epsilon'_{r,p-1} < 1)$ (Fig. 2d). It may be noted that the effects of the proximity of the helix (Fig. 2a), the permittivity value of the helix support (Fig. 2c), and the inhomogeneity parameter (Fig. 2d) are each found to be more pronounced at higher operating frequencies. The structure loading is also found to increase with the value of cotangent of the
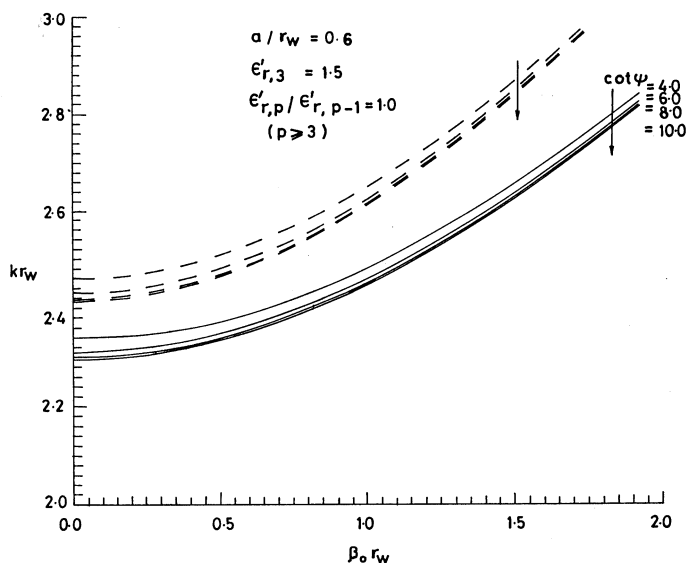
Figure 2(b).

helix pitch angle, an effect which becomes more pronounced at lower operating frequencies (Fig. 2b). It may also be noted that the dielectric parameters become less effective as the helix is brought closer to the waveguide wall and also that these parameters become more effective than the helix parameters in shaping the dispersion $(\omega \text{-} \beta)$ plot.

The azimuthal interaction impedance, for the fundamental mode $m = 0$, $K_{\theta,0}$, is plotted in Fig. 3 for a preliminary estimate of the usefulness of the structure when considered for its application in a fast-wave electron beam device such as the gyro-traveling-wave amplifier. It is observed that the value of the interaction impedance decreases as the operating frequency is increased (Fig. 3). Also, its value decreases as the helix is moved farther form the waveguide wall (Fig. 3a). The effect of the controlling parameters (namely, $a/r_w, \epsilon'_r, \epsilon'_{r,p}/\epsilon'_{r,p-1}(p \geq 3)$, etc.) on $K_{\theta,0}$ is also found to be less as the helix is brought closer to the waveguide wall (Fig. 3). Furthermore, there exists an optimum range of helix pitch angles to get a reasonable value of interaction impedance over a wide band of frequencies (Fig. 3b). The presence of the dielectric not only enhances the value of the interaction impedance but
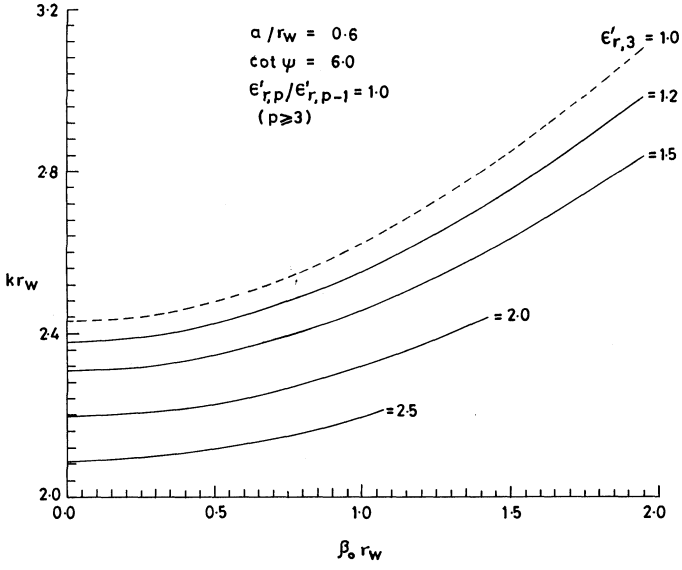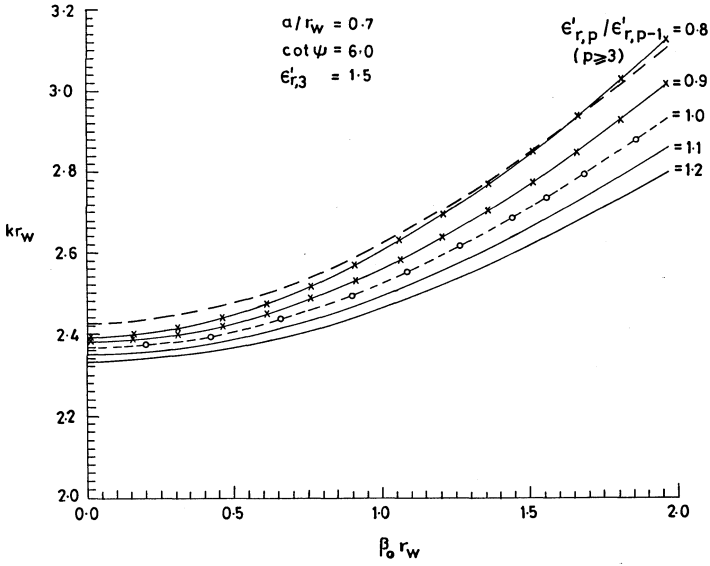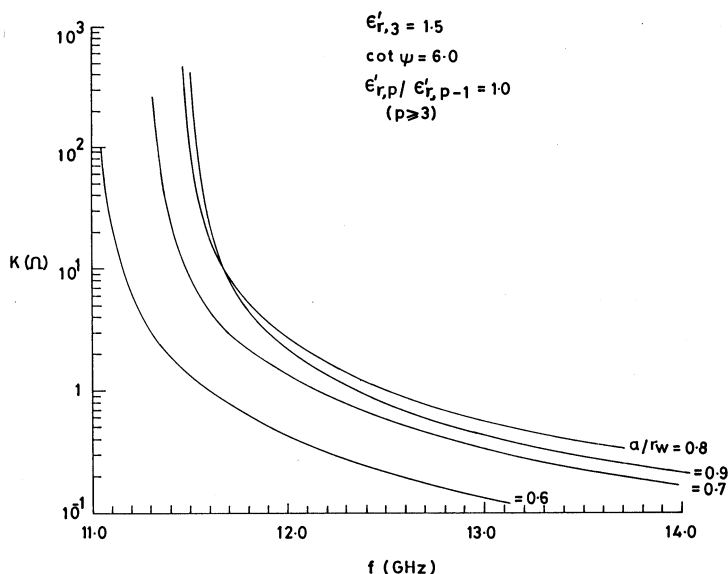
Figure 2(c).

Figure 2(d).

Figure 3(a). Interaction impedance characteristics of the structure $K \, (= K_{\theta,0})$, for the fundamental $(m = 0)$ space-harmonic mode, versus frequency f, **(a)**–**(d)** referring to the same parameters and situations as in Fig. 2, the thickness of the tape being ignored $(b_0 = a)$, though its width considered as finite at a normalized value $\delta/p = 0.3$, and the waveguide-wall radius taken as $r_w = 0.60\text{cm}$.

also reduces the rate of its fall with the increase of frequency. When the structure is dielectric loaded, the interaction impedance is found to decrease with the increase in the value of relative permittivity, the effect, however, being not discernible at higher values of the operating frequency (Fig. 3c). For an inhomogeneously-loaded structure, it is found that, if the inhomogeneity increases ($\epsilon'_{r,p}/\epsilon'_{r,p-1}(p \geq 3)$ deviating from unity), the interaction impedance increases significantly or decreases— though not so significantly, depending on whether the permittivity of the dielectric in the structure increases rapidly inward $(\epsilon'_{r,p}/\epsilon'_{r,p-1}(p \geq 3) < 1)$ or outward $(\epsilon'_{r,p}/\epsilon'_{r,p-1}(p \geq 3) > 1)$.

   In this paper the field analysis of a helix-loaded cylindrical waveguide operated in the fast-wave regime is developed in the tape-model
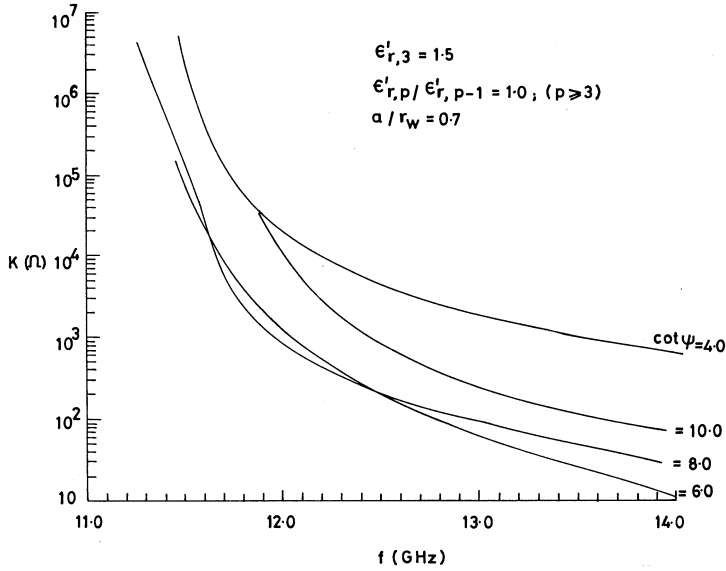
Figure 3(b).

taking care to include the effects of a generalized inhomogeneous dielectric support for the helix. The results, though it is presented here for the fundamental space-harmonic tape-helix mode and it refers to fundamental solution of the hybrid-mode, is rather general. For instance, it can be extended to the study of other space harmonic modes of interest which could be useful either in the design of a space-harmonic device of interest or in the control of undesirable space-harmonic modes. It is hoped that the present analysis should be relevant to the context of broadbanding a fast-wave electron beam device, like the gyro-TWT. The beam-wave interaction mechanism is, however, kept out of scope of the present study.
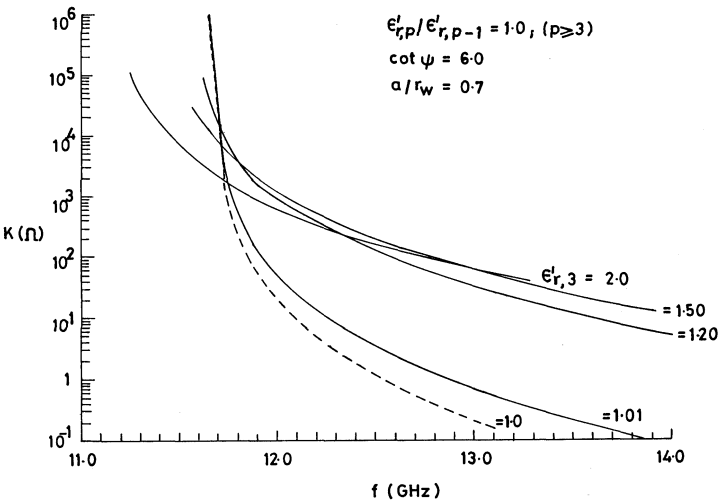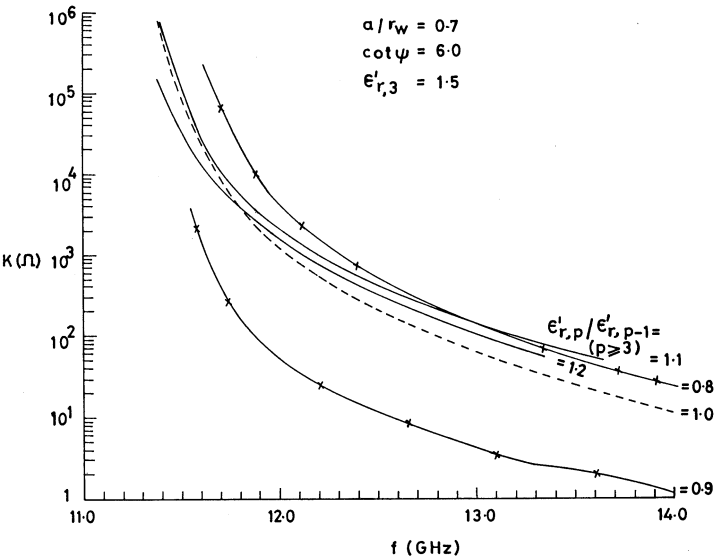
Figure 3(c).

Figure 3(d).

APPENDIX: Functions $G_{m,p}$ ($1 \le p \le n+2$) occurring in the expression (12) for interaction impedance

Functions $G_{m,p}(1 \le p \le n+2)$ occurring in the expression (12) for interaction impedance, in terms of the definite integrals defined later, are:

$$G_{m,1} = \frac{\pi \beta_m \omega \epsilon_0}{\gamma_m^2} \left(A_{m,1}^2 + \frac{\mu_0}{\epsilon_0} C_{m,1}^2 \right) \times$$

$$\int_0^a \left(J_m'^2 \{\gamma_m r\} + \frac{m^2}{\gamma_m^2 r^2} J_m^2 \{\gamma_m r\} \right) r dr,$$

$$G_{m,2} = \frac{\pi \beta_m \omega}{\gamma_m^2} \left[\left(\epsilon_0 A_{m,2}^2 + \mu_0 C_{m,2}^2 \right) \times \right.$$

$$\int_a^{b_0} \left(J_m'^2 \{\gamma_m r\} + \frac{m^2}{\gamma_m^2 r^2} J_m^2 \{\gamma_m r\} \right) r dr$$

$$+ \left(\epsilon_0 B_{m,2}^2 + \mu_0 D_{m,2}^2 \right) \times$$

$$\int_a^{b_0} \left(Y_m'^2 \{\gamma_m r\} + \frac{m^2}{\gamma_m^2 r^2} Y_m^2 \{\gamma_m r\} \right) r dr$$

$$+2 \left(\epsilon_0 A_{m,2} B_{m,2} + \mu_0 C_{m,2} D_{m,2} \right) \times$$

$$\left. \int_a^{b_0} \left(J_m' \{\gamma_m r\} Y_m' \{\gamma_m r\} + \frac{m^2}{\gamma_m^2 r^2} J_m \{\gamma_m r\} Y_m \{\gamma_m r\} \right) r dr \right]$$

and, for $3 \le p \le n+2$:

$$G_{m,p} = \frac{\pi \beta_m \omega}{\gamma_{m,p}^2} \left[\left(\epsilon_0 \epsilon_{r,p}' A_{m,p}^2 + \mu_0 C_{m,p}^2 \right) \times \right.$$

$$\int_{b_{p-3}}^{b_{p-2}} \left(J_m'^2 \{\gamma_{m,p} r\} + \frac{m^2}{\gamma_{m,p}^2 r^2} J_m^2 \{\gamma_{m,p} r\} \right) r dr$$

$$+ \left(\epsilon_0 \epsilon_{r,p}' B_{m,p}^2 + \mu_0 D_{m,p}^2 \right) \times$$

$$\int_{b_{p-3}}^{b_{p-2}} \left(Y_m'^2 \{\gamma_{m,p} r\} + \frac{m^2}{\gamma_{m,p}^2 r^2} Y_m^2 \{\gamma_{m,p} r\} \right) r dr$$

$$+ 2 \left(\epsilon_0 \epsilon_{r,p}' A_{m,p} B_{m,p} + \mu_0 C_{m,p} D_{m,p} \right) \times$$

$$\left. \int_{b_{p-3}}^{b_{p-2}} \left(J_m' \{\gamma_{m,p} r\} Y_{m,p}' \{\gamma_{m,p} r\} + \frac{m^2}{\gamma_{m,p}^2 r^2} J_m \{\gamma_{m,p} r\} Y_m \{\gamma_{m,p} r\} \right) r dr \right]$$

where

$$A_{m,1} = \zeta_1 J_{||,m}$$

and

$$C_{m,1} = \zeta_2 J_{||,m},$$

with

$$\zeta_1 = j \frac{\pi \gamma_m^2 a^2}{2\omega\epsilon_0 a} Y_m \{\gamma_m a\} \left(1 + \frac{Q_0 J_m \{\gamma_m a\}}{P_0 Y_m \{\gamma_m a\}}\right) \left(1 + \frac{m\beta_m a \cot \psi}{\gamma_m^2 a^2}\right) \sin \psi$$

and

$$\zeta_2 = (\pi/2) \gamma_m a Y_m' \{\gamma_m a\} \left(1 + \frac{N_0 J_m' \{\gamma_m a\}}{M_0 Y_m' \{\gamma_m a\}}\right) \cos \psi,$$

$$A_{m,2} = \left(\frac{J_m \{\gamma_m a\} Q_0}{P_0 Y_m \{\gamma_m a\} + Q_0 J_m \{\gamma_m a\}}\right) \zeta_1 J_{||,m}$$

$$B_{m,2} = \left(\frac{J_m \{\gamma_m a\} P_0}{P_0 Y_m \{\gamma_m a\} + Q_0 J_m \{\gamma_m a\}}\right) \zeta_1 J_{||,m}$$

$$C_{m,2} = \left(j \frac{\gamma_m}{\omega\mu_0 \cot \psi}\right) \left(\frac{J_m' \{\gamma_m a\} N_0}{M_0 Y_m' \{\gamma_m a\} + N_0 J_m' \{\gamma_m a\}}\right) \zeta_2 J_{||,m}$$

and

$$D_{m,2} = \left(j \frac{\gamma_m}{\omega\mu_0 \cot \psi}\right) \left(\frac{J_m' \{\gamma_m a\} M_0}{M_0 Y_m' \{\gamma_m a\} + N_0 J_m' \{\gamma_m a\}}\right) \zeta_2 J_{||,m};$$

for $3 \le p \le n + 1$:

$$A_{m,p} = \left(\frac{J_m \{\gamma_m a\} Q_{p-2}}{P_0 Y_m \{\gamma_m a\} + Q_0 J_m \{\gamma_m a\}}\right) \left(\prod_{q=2}^{p-1} -\frac{2\epsilon_{r,q}'}{\pi \gamma_{m,q} b_q}\right) \zeta_1 J_{||,m},$$

$$B_{m,p} = \left(\frac{J_m \{\gamma_m a\} P_{p-2}}{P_0 Y_m \{\gamma_m a\} + Q_0 J_m \{\gamma_m a\}}\right) \left(\prod_{q=2}^{p-1} -\frac{2\epsilon_{r,q}'}{\pi \gamma_{m,q} b_q}\right) \zeta_1 J_{||,m},$$

$$C_{m,p} = \left(j \frac{\gamma_m}{\omega\mu_0 \cot \psi}\right) \left(\frac{J_m' \{\gamma_m a\} N_{p-2}}{M_0 Y_m' \{\gamma_m a\} + N_0 J_m' \{\gamma_m a\}}\right)$$

$$\left(\prod_{q=2}^{p-1} -\frac{2}{\pi \gamma_{m,q} b_q}\right) \zeta_2 J_{||,m}$$

$$D_{m,p} = \left(j \frac{\gamma_m}{\omega \mu_0 \cot \psi} \right) \left(\frac{J'_m \{\gamma_m a\} M_{p-2}}{M_0 Y'_m \{\gamma_m a\} + N_0 J'_m \{\gamma_m a\}} \right)$$

$$\left(\prod_{q=2}^{p-1} -\frac{2}{\pi \gamma_{m,q} b_q} \right) \zeta_2 J_{\|,m}$$

and for $p = n + 2$:

$$A_{m,n+2} = - \left(\frac{Y_m \{\gamma_{m,n+2} c\}}{J_m \{\gamma_{m,n+2} c\}} \right) \left(\frac{J_m \{\gamma_m a\}}{P_0 Y_m \{\gamma_m a\} + Q_0 J_m \{\gamma_m a\}} \right)$$

$$\left(\prod_{q=2}^{n+1} -\frac{2\epsilon'_{r,q}}{\pi \gamma_{m,q} b_q} \right) \zeta_1 J_{\|,m},$$

$$B_{m,n+2} = \left(\frac{J_m \{\gamma_m a\}}{P_0 Y_m \{\gamma_m a\} + Q_0 J_m \{\gamma_m a\}} \right) \left(\prod_{q=2}^{n+1} -\frac{2\epsilon'_{r,q}}{\pi \gamma_{m,q} b_q} \right) \zeta_1 J_{\|,m},$$

$$C_{m,n+2} = \left(j \frac{\gamma_m}{\omega \mu_0 \cot \psi} \right) \left(\frac{Y'_m \{\gamma_{m,n+2} c\}}{J'_m \{\gamma_{m,n+2} c\}} \right)$$

$$\left(\frac{J'_m \{\gamma_m a\}}{M_0 Y'_m \{\gamma_m a\} + N_0 J'_m \{\gamma_m a\}} \right) \left(\prod_{q=2}^{n+1} -\frac{2}{\pi \gamma_{m,q} b_q} \right) \zeta_2 J_{\|,m},$$

and

$$D_{m,n+2} = \left(j \frac{\gamma_m}{\omega \mu_0 \cot \psi} \right) \left(\frac{J'_m \{\gamma_m a\}}{M_0 Y'_m \{\gamma_m a\} + N_0 J'_m \{\gamma_m a\}} \right)$$

$$\left(\prod_{q=2}^{n+1} -\frac{2}{\pi \gamma_{m,q} b_q} \right) \zeta_2 J_{\|,m}.$$

The definite integrals occuring in the above expressions for $G_{m,p}$'s are:

$$\int_x^y J_m \{\gamma_{m,p} r\} Y_m \{\gamma_{m,p} r\} \, r dr$$

$$= \left[\frac{r^2}{2} \left(\left(1 - \frac{m^2}{\gamma_{m,p}^2 r^2} \right) J_m \{\gamma_{m,p} r\} Y_m \{\gamma_{m,p} r\} \right. \right.$$

$$\left. \left. + J'_m \{\gamma_{m,p} r\} Y'_m \{\gamma_{m,p} r\} \right) \right]_x^y,$$

$$\int_x^y \left(J_m'^2 \{\gamma_{m,p}r\} + \frac{m^2}{\gamma_{m,p}^2 r^2} J_m^2 \{\gamma_{m,p}r\} \right) r\,dr$$

$$= \left[\frac{r^2}{2} \left(\frac{2 J_m \{\gamma_{m,p}r\} J_m' \{\gamma_{m,p}r\}}{\gamma_{m,p}r} + J_m'^2 \{\gamma_{m,p}r\} \right. \right.$$

$$\left. \left. + \left(1 - \frac{m^2}{\gamma_{m,p}^2 r^2} \right) J_m^2 \{\gamma_{m,p}r\} \right) \right]_x^y,$$

$$\int_x^y \left(Y_m' \{\gamma_{m,p}r\} + \frac{m^2}{\gamma_{m,p}^2 r^2} Y_m^2 \{\gamma_{m,p}r\} \right) r\,dr$$

$$= \left[\frac{r^2}{2} \left(\frac{2 Y_m \{\gamma_{m,p}r\} Y_m' \{\gamma_{m,p}r\}}{\gamma_{m,p}r} + Y_m'^2 \{\gamma_{m,p}r\} \right. \right.$$

$$\left. \left. + \left(1 - \frac{m^2}{\gamma_{m,p}^2 r^2} \right) Y_m^2 \{\gamma_{m,p}r\} \right) \right]_x^y,$$

and

$$\int_x^y \left(J_m' \{\gamma_{m,p}r\} Y_m \{\gamma_{m,p}r\} + \frac{m^2}{\gamma_{m,p}^2 r^2} J_m \{\gamma_{m,p}r\} Y_m' \{\gamma_{m,p}r\} \right) r\,dr$$

$$= \left[\frac{r^2}{2} \left(\frac{J_m' \{\gamma_{m,p}r\} Y_m \{\gamma_{m,p}r\} + J_m \{\gamma_{m,p}r\} Y_m' \{\gamma_{m,p}r\}}{\gamma_{m,p}r} \right. \right.$$

$$+ J_m' \{\gamma_{m,p}r\} Y_m' \{\gamma_{m,p}r\}$$

$$\left. \left. + \left(1 - \frac{m^2}{\gamma_{m,p}^2 r^2} \right) J_m \{\gamma_{m,p}r\} Y_m \{\gamma_{m,p}r\} \right) \right]$$

$(x, y = 0, a, b_0, b_{p-2}, b_{p-3}; 3 \le p \le n+2).$

REFERENCES

1. Neureuther, R., P. W. Klock, and R. Mittra, "A study of the sheath helix with a conducting core and its applications to the helical antenna," *IEEE Trans. Antennas and Propagation,* Vol. AP-15, 203–210, 1967.
2. Watkins, D. A., *Topics in Electromagnetic Theory,* Wiley, New York, 1958.
3. Hagmann, M. J., "Propagation of sheath helix in a coaxially layered lossy dielectric medium," *IEEE Trans. Microwave Theory & Tech.,* Vol. MTT-32, 122–126, 1984.

4. McMurtry, J. B., "Fundamental interaction impedance of a helix surrounded by a dielectric and a metal shield," *IRE Trans. Electron Devices,* Vol. ED-9, 210–216, 1962.

5. Paik, S. F., "Design formulas for helix dispersion shaping," *IEEE Trans. Electron Devices,* Vol. ED-16, 1010–1014, 1969.

6. Tsutaki, K., Y. Yuasa, and Y. Morizumi, "Numerical analysis and design for high-performance helix traveling-wave tubes," *IEEE Trans. Electron Devices,*, Vol. ED-32, 1842–1849, 1985.

7. Basu, B. N., and A. K. Sinha, "Dispersion-shaping using an inhomogeneous dielectric support for the helix in travelling-wave tube," *Int. J. Electronics,* Vol. 50, 235–238, 1981.

8. Basu, B. N., R. K. Jha, A. K. Sinha, and L. Kishore, "Electromagnetic wave propagation through an azimuthally perturbed helix," *J. Appl. Phys.,* Vol. 58, 3625–3627, 1985.

9. Uhm, H. S., and J. Y. Choe, "Properties of the electromagnetic wave propagation in a helix-loaded waveguide," *J. Appl. Phys.,* Vol. 53, 8483–8488, 1982.

10. ———— , "Electromagnetic-wave propagation in a conducting waveguide loaded with a tape helix," *IEEE Trans. Microwave Theory & Tech.,* Vol. MTT-31, 704–709, 1983.

11. ———— , "Theory of gyrotron amplifier in a helix loaded waveguide," *J. Appl. Phys.,* Vol. 54, 4889–4894, 1983.

12. Sensiper, S., "Electromagnetic wave propagation on helical structures," *Proc. IRE,* Vol. 43, 149–161, 1955.

14. Tien, P. K., "Traveling-wave tube helix impedance," *Proc. IRE,* Vol. 41, 1617–1623, 1953.

14. Grow, R. W., and U. A. Srivastava, "Impedance calculations for travelling wave gyrotron operating at harmonics of cyclotron frequency in magnetron-type circuits," *Int. J. Electronics,* Vol. 53, 699–707, 1982.

15. Sangster, A. J., "Small-signal analysis of the travelling-wave gyrotron using Pierce parameters," *Proc. IEE,* Vol. 127, Pt. I, 45–52, 1980.

16. Jain, P. K., and B. N. Basu, "The inhomogeneous loading effects of practical dielectric supports for the helical slow-wave structure of a TWT," *IEEE Trans. Electron Devices,* Vol. ED-34, 2643–2648, 1987.

17. Pierce, J. R., *Traveling-Wave Tubes,* Van Nostrand, New York, 1950.

18. Swift-Hook, D. T., "Dispersion curves for a helix in glass tube," *Proc. IEE,* Vol. 150b supp., 747–755, 1958.

19. Ghosh, S., P. K. Jain, and B. N. Basu, "Analytical exploration of new tapered-geometry dielectric-supported helix slow-wave structures for broadband TWT's," *Progress in Electromagnetics Research,* Vol. PIER 15, 63–85, 1997.

20. Ghosh, S., P. K. Jain, and B. N. Basu, "Rigorous tape analysis of inhomogeneously loaded helical slow-wave structures," *IEEE Trans. Electron Devices,* Vol. ED-44, to be published in June 1997 issue.